Received: 26 July 2018 | Revised: 21 May 2019 | Accepted: 31 May 2019

DOI: 10.1002/sim.8287

RESEARCH ARTICLE

WILEY Statistics in Medicine

Assessing the impact of sleep time on truck driver performance using a recurrent event model

Yi Liu[1] | **Feng Guo**[1,2] | **Richard J. Hanowski**[2]

[1]Department of Statistics, Virginia Tech, Blacksburg, Virginia

[2]Virginia Tech Transportation Institute, Virginia Tech, Blacksburg, Virginia

Correspondence
Feng Guo, Department of Statistics, Virginia Tech, Blacksburg, VA 24061.
Email: feng.guo@vt.edu

Driver fatigue is a major safety concern for commercial truck drivers and is directly related to the total hours of sleep prior to a working shift. To evaluate changes in driving performance over a long on-duty driving period, we propose a mixed Poisson process recurrent-event model with time-varying coefficients. We use data from 96 commercial truck drivers whose trucks were instrumented with an advanced in situ data acquisition system. The driving performance is measured by unintentional lane deviation events, a known performance deterioration related to fatigue. Driver sleep time and other activities are extracted from a detailed activity register. The time-varying coefficients are used to model the baseline intensity and difference among three cohorts of shifts in which the driver slept less than 7 hours, between 7 to 9 hours, and more than 9 hours prior to driving. We use the penalized B-splines approach to model the time-varying coefficients and an expectation-maximization algorithm with embedded penalized quasi-likelihood approximation for parameter estimation. Simulation studies show that the proposed model fits low and high event rate data well. The results show a significantly higher intensity after 8 hours of on-duty driving for shifts with less than 7 hours of sleep prior to work. The study also shows drivers tend to self-adjust sleep duration, total driving hours, and breaks. This study provides crucial insight into the impact of sleep time on driving performance for commercial truck drivers and highlights the on-road safety implications of insufficient sleep and breaks while driving.

KEYWORDS

driving fatigue, penalized splines, recurrent event models, time-varying coefficients, truck driving safety

1 | INTRODUCTION

Traffic crashes are a major safety hazard for commercial truck drivers and are also a general public health concern. In 2015, heavy trucks were involved in 3598 fatal crashes in the United States, which led to 667 truck driver fatalities and 4067 total fatalities.[1] In addition, 116 000 persons were injured due to heavy vehicle crashes. In the United States, the operational hours for commercial truck drivers are regulated by the Federal Motor Carrier Safety Administration. Referred to as the hours-of-service (HOS) regulations, truck drivers can work 14 hours, 11 hours of which can be driving, before taking a 10-hour off-duty break.[2] Although not all drivers may work the fully allocated 14 hours, or drive the allocated 11 hours, for drivers that do push the work/driving limits (eg, long-haul truck drivers), fatigue is a major risk factor.[3] Fatigue issues associated with time-on-task and deterioration of driving performance over the course of a long work day or drive are of particular concern for this cohort. Although the importance of being well-rested for optimal performance has been

documented,[4] there has been limited research to evaluate the change in driving performance and safety risk over time as a function of preshift sleep time.

Many factors can affect driver fatigue, including total sleep time, sleep debt, circadian rhythm, breaks during long shifts, and caffeine intake. Among these factors, sleep time the night before driving has been noted as a critical risk factor.[5] Being well rested prior to a long shift has a direct impact on driver fatigue and driving performance.[4,6,7] Insufficient sleep is typically defined as sleep less than 7 hours per day.[8-12] Sleep debt, the cumulative lack of sleep for a period of time, also negatively affects driver fatigue.[13,14] Furthermore, it has also been shown that breaks during a long shift reduce the number of on-road safety-critical events for truck drivers.[15]

Traffic safety modeling is a challenging research area due to complex nature of crashes.[16-18] Many factors contribute to crash risk including driver behavior, traffic condition, environmental factors, and vehicle factors. Driver behavior, such as distraction and impairment, has been a major risk factor for traffic safety.[19-21] A study by the National Highway Traffic Safety Administration indicates that human error was the critical reason for 93% of crashes.[22] The recent advancement in data collection methods, in particular, the naturalistic driving study (NDS) method, have provided unprecedented opportunity to evaluate driver behavior and risk but also bring challenges due to complex data structure.[23] Novel statistical approaches have been developed to model such data.[24,25]

Recurrent event data are commonly observed in clinical trials and epidemiological studies in which individuals can experience repeated events of interest over the study period. Examples include multiple occurrences of bladder tumors for patients in bladder cancer trials,[26] multiple mammary tumors for animals in carcinogenicity experiments,[27] and recurrent pulmonary exacerbations for patients with cystic fibrosis.[28] One typical feature of recurrent events is that event times within the same subject are correlated. Common approaches for recurrent event data analysis include marginal models based on estimating functions[29-31] and conditional models based on frailty distributions.[32-34] Methods using estimating functions are to directly model marginal means and treat the dependence structure of events as nuisance parameters. In contrast, conditional models use frailty distributions to characterize the heterogeneity and correlation among events, and allow both marginal and conditional inferences.

Driver often experience various type of safety events, eg, crashes, near-crashes, safety critical events, and unintentional lane deviation (ULD).[35-37] These events are rarely terminal and often occur at different frequencies, depending on the severity and nature of the events. Recurrent event models can provide valuable insight into the latent temporal driving profile.[38] used recurrent event models to evaluate the impact of crashes on driver behavior measured by safety critical events. Recurrent-event models have been used to identify the risk change point of novice teenage drivers.[39,40] As driving performance is likely to change over a long shift, it is expected that such change will reflected in certain types of recurrent events.

The effect of a covariate in recurrent event data analysis may not be constant over time. For this study, the temporal profile of preshift sleep time affecting subsequent driving performance is of key interest for fatigue management and HOS regulations. Varying coefficient models for longitudinal data include kernel-based approaches[41,42] and spline-based approaches.[43] Kernel estimators are constructed through a weighted mean of the nearby observations and have great intuitive appeal. However, the kernel weights are asymmetric at boundaries of the predictor space and could cause substantial bias for the estimate.[44] Spline estimators are based on linear combinations of piecewise polynomial functions. The computations are relatively fast and can be easily implemented.[45] Varying coefficient models have also been studied in the recurrent event data setting.[46-48] However, they are based on the partial likelihood approach,[49] in which the baseline intensity is considered as a nuisance parameter and not explicitly estimated. For this study, driving performance is likely to change over a long shift due to fatigue and other factors. Therefore, smooth estimation of the baseline intensity needs to be incorporated to characterize the time-changing pattern of driving performance.

This paper develops a mixed Poisson process model with time-varying coefficients for recurrent event data. The correlation among event times is characterized by using gamma frailties. The approach of penalized B-splines[45] is used for modeling both the log baseline intensity and time-varying coefficients. For penalized splines, the fit is conditional on the smoothing parameter, which has to be selected by cross-validation or optimizing some performance criterion. These procedures could be computationally demanding as the number of time-varying coefficients increases. To address the issue, we adopt a mixed-model representation approach based on the connection between penalized likelihood and random effect models.[50-53] Spline coefficients are treated as random effects and smoothing parameters are estimated as variance components. An expectation-maximization (EM) algorithm is used to fit the model, in which the penalized quasi-likelihood (PQL) approach[54] is adopted for likelihood approximation.

The rest of this paper is arranged as follows. In Section 2, we introduce the mixed Poisson process model with time-varying coefficients as well as the mixed-model representation of penalized splines. The model performance is

evaluated by a simulation study presented in Section 3. In Section 4, we apply the proposed model to the Commercial Truck Driver NDS and evaluate how the preshift sleep duration affects the temporal profile of the intensity of ULD events. Summary and discussion are presented in Section 5.

2 | METHODOLOGY

We propose a mixed Poisson process model with time-varying coefficients in a recurrent event data setting. Both the log baseline intensity and time-varying coefficients are modeled by penalized B-splines. A mixed-model representation of penalized splines is adopted to estimate the amount of smoothness for the spline fit.

2.1 | Model

Consider a sample of I shifts. Let $\{N_i(t), t \geq 0\}$ be a right-continuous counting process that records the number of events over driving time $[0, t]$ in shift i. Let $\boldsymbol{x_i} = (x_{i1}, \ldots, x_{ip})'$ denote a covariate vector with constant coefficients, and $\boldsymbol{z_i} = (z_{i1}, \ldots z_{iq})'$ denote a covariate vector with time-varying coefficients. Given a random effect u_i, $\{N_i(t), t \geq 0\}|\boldsymbol{x_i}, \boldsymbol{z_i}, u_i$ is assumed to be an independent Poisson process with conditional intensity function as

$$\lambda_i(t|\boldsymbol{x_i}, \boldsymbol{z_i}, u_i) = u_i \exp\left\{\boldsymbol{x_i'\alpha} + \beta_0(t) + z_{i1}\beta_1(t) + \cdots + z_{iq}\beta_q(t)\right\}. \tag{1}$$

$\boldsymbol{\alpha}$ is a vector of unknown regression coefficients and $\boldsymbol{x_i'\alpha}$ represents the linear component of the log intensity. $\beta_0(t), \beta_1(t), \ldots, \beta_q(t)$ are unknown smooth functions, ie, $\beta_0(t)$ is the log baseline intensity and the rest are time-varying coefficients of the covariates in $\boldsymbol{z_i}$. This paper assumes that u_i follows an independent and identical gamma distribution with density $p(u_i; \phi)$, where $\mathrm{E}(u_i) = 1$ and $\mathrm{var}(u_i) = \phi$. Large values of ϕ indicate greater heterogeneity between shifts and stronger association among event times.

Let t_{ij} denote the driving time to the jth event that occurred in shift i. Suppose $n_i(\geq 0)$ events are observed in shift i at driving times $0 < t_{i1} < \ldots < t_{i,n_i}$ before the censoring time c_i. Let $\boldsymbol{D_i^{\mathrm{obs}}}$ denote the observed data for shift i, including event times, censoring time, and covariate values. The log likelihood given the complete data $\boldsymbol{D_i^{\mathrm{obs}}}, u_i, 1 \leq i \leq I\}$ is

$$l_{\mathrm{c}} = \sum_{i=1}^{I}\left\{\sum_{j=1}^{n_i}[\log u_i + \log \rho_i(t_{ij})] - u_i\mu_i(c_i)\right\} + \sum_{i=1}^{I}\log p(u_i; \phi), \tag{2}$$

with $\rho_i(t) = \exp\{\boldsymbol{x_i'\alpha} + \beta_0(t) + z_{i1}\beta_1(t) + \ldots + z_{iq}\beta_q(t)\}$ and $\mu_i(c_i) = \int_0^{c_i}\rho_i(t)\mathrm{d}t$. By integrating u_i's from the complete-data likelihood, we obtain the log marginal likelihood as

$$l_{\mathrm{m}} = \sum_{i=1}^{I}\sum_{j=1}^{n_i}\log\rho_i(t_{ij}) - \sum_{i=1}^{I}\left(n_i + \frac{1}{\phi}\right)\log(1 + \phi\mu_i(c_i)) + \sum_{i=1}^{I}\sum_{j=0}^{n_i^*}\log(1 + j\phi), \tag{3}$$

with $n_i^* = \max(0, n_i - 1)$. The integral $\mu_i(c_i)$ in likelihood functions (2) and (3) is based on $\beta_0(t), \beta_1(t), \ldots, \beta_q(t)$. Since there is no analytic solution, we use the trapezoid method to approximate the integral. Consider a grid of points $0 = s_0 < s_1 < \ldots < s_m = t_{\max}$ over the domain of time. For shift i, define index $m_i = \min\{k : s_k \geq c_i\}$. Then, $\mu_i(c_i)$ can be approximated by a polygon going through the points $(s_k, \rho_i(s_k))$, for $0 \leq k \leq m_i - 1$. The approximation yields

$$\begin{aligned}\mu_i(c_i) &\approx (c_i - s_{m_i-1})\frac{\rho_i(s_{m_i}) + \rho_i(s_{m_i-1})}{2} + I(m_i \geq 2)\sum_{k=1}^{m_i-1}(s_k - s_{k-1})\frac{\rho_i(s_k) + \rho_i(s_{k-1})}{2}\\ &= \frac{1}{2}\min(c_i, s_1)\rho_i(s_0) + \frac{1}{2}\sum_{k=1}^{m_i}[\min(c_i, s_{k+1}) - \min(c_i, s_{k-1})]\rho_i(s_k),\end{aligned}$$

where $I(\cdot)$ denotes the indicator function.

To model the baseline intensity and time-varying coefficients, we assume that $\beta_l(t), 0 \leq l \leq q$, can be approximated by polynomial splines of degree v with equally spaced knots $0 = \zeta_{l0} < \zeta_{l1} < \cdots < \zeta_{l,k_l} = t_{\max}$ over the domain of time.

Let $B_{lk}(t)$ denote the value at t of the kth B-spline, and $\boldsymbol{B_l}(t) = (B_{l1}(t), \ldots, B_{l,K_l}(t))'$ denote $K_l = k_l + v$ B-spline basis functions. The parameterization used for the splines is

$$\beta_l(t) = \sum_{k=1}^{K_l} \beta_{lk} B_{lk}(t) = \boldsymbol{B_l'}(t)\boldsymbol{\beta_l}. \tag{4}$$

$\boldsymbol{\beta_l} = (\beta_{l1}, \ldots, \beta_{l,K_l})'$ is a vector of unknown regression coefficients for the splines. To ensure sufficient flexibility for the spline fit, a moderately large number of knots should be chosen. However, this could lead to severe overfitting. Eilers and Marx[45] proposed a penalized approach to prevent overfitting by incorporating a difference penalty on the coefficients of adjacent splines. Let Δ denote the difference operator so that the first-order difference of β_{lk} is $\Delta\beta_{lk} = \beta_{lk} - \beta_{l,k-1}$, the second-order difference is $\Delta^2\beta_{lk} = \Delta(\Delta\beta_{lk}) = \beta_{lk} - 2\beta_{l,k-1} + \beta_{l,k-2}$, and so on. In general, a difference penalty based on the rth-order difference is subtracted from the log likelihood; parameters are estimated by maximizing the resulting penalized likelihood function, ie,

$$l_c - \sum_{l=0}^{q} \left\{ \frac{\lambda_l}{2} \sum_{k=r+1}^{K_l} (\Delta^r \beta_{lk})^2 \right\}. \tag{5}$$

λ_l, often known as the smoothing parameter, is a nonnegative constant, which can be adjusted to control the smoothness of the fit.

To estimate the smoothing parameter, we adopt a mixed-model representation of penalized splines based on the connection between penalized likelihood and random effects models.[50-53] Cai et al[55] and Cai and Betensky[56] employed such connection in baseline hazard estimation and treated the coefficients of truncated power splines as independent Gaussian random effects. For B-splines used in this paper, we assume that the rth-order difference $\Delta^r\beta_{lk}$, $r+1 \le k \le K_l$, is a random effect following an independent and identical normal distribution $N(0, 1/\tau_l)$. Let $\boldsymbol{D_l}$ be a matrix such that $\boldsymbol{D_l}\boldsymbol{\beta_l} = (\Delta^r\beta_{l,r+1}, \ldots, \Delta^r\beta_{l,K_l})'$. The probability density of $\boldsymbol{\beta_l}$ can be written as

$$p(\boldsymbol{\beta_l}; \tau_l) \propto \tau_l^{(K_l - r)/2} \exp\left\{ -\frac{\tau_l}{2} \boldsymbol{\beta_l} \left(\boldsymbol{D_l'D_l} \right) \boldsymbol{\beta_l} \right\}. \tag{6}$$

The smoothness of the fit is now controlled by the inverse variance τ_l, which corresponds to λ_l in the penalized likelihood approach. It should be noted that formulation (6) is originally proposed as a prior in the Bayesian approach to penalized splines.[57,58] Yet in the frequentist setting by assuming spline coefficients to be random, smoothing parameter selection turns into inverse variance estimation. In the following section, we show that, with the PQL method,[54] the estimate is approximately equivalent to a penalized spline fit under a certain amount of difference penalty.

2.2 | Estimation

The model is fitted by a variation of EM algorithm with the PQL approach embedded for likelihood approximation. Let $\tilde{l}$ denote the likelihood functions in which $\boldsymbol{\beta_l}$ is random with density (6). The log likelihood given the complete data $\{\boldsymbol{D_i^{obs}}, u_i, 1 \le i \le I, \boldsymbol{\beta_l}, 0 \le l \le q\}$ is

$$\begin{aligned} \tilde{l}_c &= \sum_{i=1}^{I} \left\{ \sum_{j=1}^{n_i} [\log u_i + \log \rho_i(t_{ij})] - u_i \mu_i(c_i) \right\} + \sum_{i=1}^{I} \log p(u_i; \phi) + \sum_{l=0}^{q} \log p(\boldsymbol{\beta_l}; \tau_l) \\ &= \tilde{l}_1(\boldsymbol{\alpha}, \boldsymbol{\tau}) + \tilde{l}_2(\phi), \end{aligned}$$

where $\boldsymbol{\tau} = (\tau_0, \tau_1, \ldots, \tau_q)'$,

$$\tilde{l}_1(\boldsymbol{\alpha}, \boldsymbol{\tau}) = \frac{1}{2} \sum_{l=0}^{q} (K_l - r) \log \tau_l + \sum_{i=1}^{I} \sum_{j=1}^{n_i} \log \rho_i(t_{ij}) - \sum_{i=1}^{I} u_i \mu_i(c_i) - \frac{1}{2} \boldsymbol{\beta}' \boldsymbol{P}(\boldsymbol{\tau}) \boldsymbol{\beta},$$

and

$$\tilde{l}_2(\phi) = \frac{1}{\phi}\sum_{i=1}^{I}(\log u_i - u_i) + I\left[\frac{1}{\phi}\log\left(\frac{1}{\phi}\right) - \log\Gamma\left(\frac{1}{\phi}\right)\right].$$

$\boldsymbol{\beta}' = (\boldsymbol{\beta_0}', \boldsymbol{\beta_1}', \ldots, \boldsymbol{\beta_q}')$, and $\boldsymbol{P}(\boldsymbol{\tau})$ is a block diagonal matrix with block $\tau_l(\boldsymbol{D_l}'\boldsymbol{D_l})$ in the term corresponding to $\boldsymbol{\beta_l}$ and 0's elsewhere.

In the E-step of the algorithm, conditional on the observed data, u_i independently follows a gamma distribution, with shape parameter $A_i = n_i + 1/\phi$ and rate parameter $B_i = \mu_i(c_i) + 1/\phi$. Given the data and the current values of A_i and B_i, the expectation of $\tilde{l}_c$ with respect to u_i is $\tilde{Q}_1(\boldsymbol{\alpha}, \boldsymbol{\tau}) + \tilde{Q}_2(\phi)$, where

$$\tilde{Q}_1(\boldsymbol{\alpha}, \boldsymbol{\tau}) = \frac{1}{2}\sum_{l=0}^{q}(K_l - r)\log\tau_l + \sum_{i=1}^{I}\sum_{j=1}^{n_i}\log\rho_i(t_{ij}) - \sum_{i=1}^{I}\left(\frac{A_i}{B_i}\right)\mu_i(c_i) - \frac{1}{2}\boldsymbol{\beta}'\boldsymbol{P}(\boldsymbol{\tau})\boldsymbol{\beta},$$

and

$$\tilde{Q}_2(\phi) = \frac{1}{\phi}\sum_{i=1}^{I}\left(\psi(A_i) - \log(B_i) - \frac{A_i}{B_i}\right) + I\left[\frac{1}{\phi}\log\left(\frac{1}{\phi}\right) - \log\Gamma\left(\frac{1}{\phi}\right)\right].$$

$\psi(\cdot)$ denotes the digamma function.

In the M-step of the algorithm, we can update the value of ϕ by maximizing $\tilde{Q}_2$. To update the estimates of $(\boldsymbol{\alpha}, \boldsymbol{\tau})$, it is important to notice that $\tilde{Q}_1$ is conditional on the random effects $\boldsymbol{\beta_l}$'s. Therefore, $\boldsymbol{\beta_l}$'s need to be integrated out. The integrated $\tilde{Q}_1$ is

$$\log\int\exp\tilde{Q}_1\,\mathrm{d}\boldsymbol{\beta} = \frac{1}{2}\sum_{l=0}^{q}(K_l - r)\log\tau_l + \log\int\exp\{-\kappa(\boldsymbol{\beta})\}\,\mathrm{d}\boldsymbol{\beta}, \tag{7}$$

where

$$-\kappa(\boldsymbol{\beta}) = \sum_{i=1}^{I}\sum_{j=1}^{n_i}\log\rho_i(t_{ij}) - \sum_{i=1}^{I}\left(\frac{A_i}{B_i}\right)\mu_i(c_i) - \frac{1}{2}\boldsymbol{\beta}'\boldsymbol{P}(\boldsymbol{\tau})\boldsymbol{\beta}. \tag{8}$$

Since there is no closed form for the integral in (7), we apply Laplace's method[59] for approximation. Let κ' and κ'' denote the first and second partial derivative of κ with respect to $\boldsymbol{\beta}$. The approximation yields

$$\log\int\exp\tilde{Q}_1\,\mathrm{d}\boldsymbol{\beta} \approx \frac{1}{2}\sum_{l=0}^{q}(K_l - r)\log\tau_l - \frac{1}{2}\log|\kappa''(\tilde{\boldsymbol{\beta}})| - \kappa(\tilde{\boldsymbol{\beta}}), \tag{9}$$

where $\tilde{\boldsymbol{\beta}} = \tilde{\boldsymbol{\beta}}(\boldsymbol{\alpha}, \boldsymbol{\tau})$ is the solution to $\kappa'(\boldsymbol{\beta}) = \mathbf{0}$ that maximizes $-\kappa(\boldsymbol{\beta})$. We follow the work of Breslow and Clayton[54] in their PQL approach for generalized linear mixed models. That is, we ignore the first two terms in (9) and choose $\boldsymbol{\alpha}$ to maximize $-\kappa(\tilde{\boldsymbol{\beta}})$. Consequently, $(\hat{\boldsymbol{\alpha}}(\boldsymbol{\tau}), \hat{\boldsymbol{\beta}}(\boldsymbol{\tau}))$, where $\hat{\boldsymbol{\beta}}(\boldsymbol{\tau}) = \tilde{\boldsymbol{\beta}}(\hat{\boldsymbol{\alpha}}(\boldsymbol{\tau}))$, jointly maximizes $-\kappa(\boldsymbol{\beta})$. If $\boldsymbol{\tau}$ was known and $\boldsymbol{\beta_l}$'s were fixed effects, $-\kappa(\boldsymbol{\beta})$ would be the penalized likelihood with $-(1/2)\boldsymbol{\beta}'\boldsymbol{P}(\boldsymbol{\tau})\boldsymbol{\beta}$ being equivalent to the difference penalty term in (5). The PQL approximation implies that, given $\boldsymbol{\tau}$, maximizing the integrated $\tilde{Q}_1$ is approximately equivalent to maximizing the penalized likelihood. The estimation procedure is then reduced to solving the score equation of $-\kappa(\boldsymbol{\beta})$ for $(\boldsymbol{\alpha}, \boldsymbol{\beta})$, and the Newton-Raphson algorithm can be applied.

By assigning the maximized values $(\hat{\boldsymbol{\alpha}}(\boldsymbol{\tau}), \hat{\boldsymbol{\beta}}(\boldsymbol{\tau}))$ back into (9), we obtain an approximate profile likelihood of $\boldsymbol{\tau}$ as

$$\frac{1}{2}\sum_{l=0}^{q}(K_l - r)\log\tau_l - \frac{1}{2}\log|\kappa''(\hat{\boldsymbol{\beta}})| - \frac{1}{2}\hat{\boldsymbol{\beta}}'\boldsymbol{P}(\boldsymbol{\tau})\hat{\boldsymbol{\beta}}. \tag{10}$$

Differentiation of (10) with respect to τ_l gives the following estimating equation:

$$\frac{1}{2}\left[\frac{K_l - r}{\tau_l} - \mathrm{tr}\left(\kappa''(\hat{\boldsymbol{\beta}})^{-l}\boldsymbol{D_l}'\boldsymbol{D_l}\right) - \hat{\boldsymbol{\beta}}_{\boldsymbol{l}}'\left(\boldsymbol{D_l}'\boldsymbol{D_l}\right)\hat{\boldsymbol{\beta}}_{\boldsymbol{l}}\right] = 0,$$

where $\mathrm{tr}(\cdot)$ is the trace operation of a matrix, and $\kappa''(\hat{\boldsymbol{\beta}})^{-l}$ is the diagonal block corresponding to $\boldsymbol{\beta_l}$ in $\kappa''(\hat{\boldsymbol{\beta}})^{-1}$. The solution is of the simple form

$$\hat{\tau}_l = \frac{K_l - r}{\mathrm{tr}\left(\kappa''(\hat{\boldsymbol{\beta}})^{-l}\boldsymbol{D_l}'\boldsymbol{D_l}\right) + \hat{\boldsymbol{\beta}}_{\boldsymbol{l}}'\left(\boldsymbol{D_l}'\boldsymbol{D_l}\right)\hat{\boldsymbol{\beta}}_{\boldsymbol{l}}}. \tag{11}$$

The estimation procedure can be conducted in two steps. First, a set of random initial values were assigned to $(\boldsymbol{\alpha}, \boldsymbol{\beta}, \boldsymbol{\tau}, \phi)$. Conditional on the current values, we update ϕ by maximizing $\widetilde{Q}_2$ and update $(\boldsymbol{\alpha}, \boldsymbol{\beta})$ by solving the score equation of $-\kappa(\boldsymbol{\beta})$. Second, through the updated values of $\boldsymbol{\alpha}$ and $\boldsymbol{\beta}$, we obtain a new value for τ_l using (11). These two steps are iterated until convergence.

After obtaining estimates for $\boldsymbol{\theta} = (\boldsymbol{\alpha}, \boldsymbol{\beta}, \phi)$, we follow the similar method by Gray[60] and obtain the covariance matrix of $\hat{\boldsymbol{\theta}} - \boldsymbol{\theta}$ given $\boldsymbol{\tau}$ approximately as

$$\operatorname{cov}\left(\left[\begin{array}{c}\hat{\boldsymbol{\alpha}}\\ \hat{\boldsymbol{\beta}} - \boldsymbol{\beta}\\ \hat{\phi}\end{array}\right]\middle\| \boldsymbol{\tau}\right) = [\boldsymbol{I}(\boldsymbol{\theta}) + \boldsymbol{P}(\boldsymbol{\tau})]^{-1}\boldsymbol{I}(\boldsymbol{\theta})[\boldsymbol{I}(\boldsymbol{\theta}) + \boldsymbol{P}(\boldsymbol{\tau})]^{-1}, \tag{12}$$

where $\boldsymbol{I}(\boldsymbol{\theta}) = -\partial^2 l_{\mathrm{m}}(\boldsymbol{\theta})/\partial\boldsymbol{\theta}^2$ and l_{m} is the log marginal likelihood defined in (3). To obtain the confidence interval for $\hat{\beta}_l(t)$, we estimate the variance of $\hat{\beta}_l(t)$ as $\widehat{\operatorname{var}}[\hat{\beta}_l(t)] = \boldsymbol{B}_{\boldsymbol{l}}'(t)\widehat{\operatorname{cov}}(\hat{\boldsymbol{\beta}} - \boldsymbol{\beta}|\boldsymbol{\tau})\boldsymbol{B}_{\boldsymbol{l}}(t)$. It should be noted that, as the uncertainty in estimating $\boldsymbol{\tau}$ is ignored in (12), these estimates tend to underestimate the true variances; however, the source of variation due to the estimation of $\boldsymbol{\tau}$ is negligible for large samples.[56] The potential influence is evaluated in the simulation study in Section 3.

3 | SIMULATION

We conducted a simulation study to evaluate the model performance. Two major factors could affect the fitting results are the curvature of time-varying coefficients and the magnitude of event rate. We generated data from low and high event rates with time-varying coefficients of different curvatures.

Simulated data were generated from a Poisson process with conditional intensity function

$$\lambda_i(t|u_i) = u_i \exp\{x_{i1}\alpha_1 + \beta_0(t) + z_{i1}\beta_1(t) + z_{i2}\beta_2(t)\},\ 0 < t \le 10.$$

We considered $I = 500$ shifts. The censoring time c_i was generated from a gamma distribution independent of the shift. Shifts were censored at the maximum follow-up time, 10, if not censored before. u_i's were generated from a gamma distribution with mean of 1 and variance $\phi = 5$. The covariate x_{i1} was generated from a uniform distribution on $[-1, 1]$, and its coefficient was $\alpha_1 = 0.5$. The covariates z_{i1} and z_{i2} were binary with probability distribution $p(z_{i1}, z_{i2}) = (1 - p_1 - p_2)^{1-z_{i1}-z_{i2}} p_1^{z_{i1}} p_2^{z_{i2}}$, where $0 \le z_{i1} + z_{i2} \le 1$ and $p_1 = p_2 = 1/3$. There were two settings for the time-varying coefficients. Setting 1 considered functions of low curvature (shown in Figure 1)

$$\begin{aligned}\beta_1(t) &= \frac{10}{1 + e^{-0.4(t-3)}} + \frac{10}{1 + e^{0.4(t-6)}} - 12.5,\\ \beta_2(t) &= \sin(0.2\pi t).\end{aligned}$$

Setting 2 considered functions of high curvature (shown in Figure 2)

$$\begin{aligned}\beta_1(t) &= \frac{8}{1 + e^{-(t-4.5)}} + \frac{8}{1 + e^{(t-5.5)}} - 9,\\ \beta_2(t) &= \frac{15}{1 + e^{-(t-4)}} + \frac{15}{1 + e^{(t-4.5)}} + \frac{15}{1 + e^{(t-5.5)}} + \frac{15}{1 + e^{-(t-6)}} - 30.\end{aligned}$$

There were two settings for the log baseline intensity, ie, a low event rate setting with $\beta_0(t) = 0.1t - 2.75$ and a high event rate setting with $\beta_0(t) = 0.1t - 1.5$.

We generated 500 data sets under each setting. The average number of events per shift (shown in Table 1) was 0.8 for the low event rate setting and 3 for the high event rate setting. $\beta_l(t)$'s were approximated using cubic B-splines with the number of knots $k_l = 10$ and the difference penalty order $r = 3$. Each data set was fitted in two approaches, ie, (1) using splines for both $\beta_l(t)$'s and α_1 and (2) using splines for $\beta_l(t)$'s only.

Simulation results for the spline fit are shown in Figures 1 and 2. For time-varying coefficients of low curvature, the mean of spline estimate shows very little bias, and the pointwise coverage probability is close to 95% over most of the follow-up period. For time-varying coefficients of high curvature, the mean estimates of $\beta_1(t)$ and $\beta_2(t)$ show larger bias

TABLE 1 Simulation: parametric coefficient estimates

Curvature	Number of events per shift	Fit		True	Mean	Bias	SE	SEM	CP (%)
low	0.83	1	ϕ	5	4.91	−0.09	0.68	0.65	
	(low event rate)	2	α_1	0.5	0.49	−0.01	0.19	0.20	96.2
			ϕ	5	4.91	−0.09	0.68	0.65	
	2.93	1	ϕ	5	4.97	−0.03	0.46	0.46	
	(high event rate)	2	α_1	0.5	0.50	0.00	0.18	0.18	95.6
			ϕ	5	4.97	−0.03	0.46	0.46	
high	0.86	1	ϕ	5	4.90	−0.10	0.65	0.64	
	(low event rate)	2	α_1	0.5	0.49	−0.01	0.20	0.20	94.4
			ϕ	5	4.90	−0.10	0.65	0.64	
	2.99	1	ϕ	5	4.97	−0.03	0.47	0.46	
	(high event rate)	2	α_1	0.5	0.50	−0.00	0.18	0.18	95.6
			ϕ	5	4.97	−0.03	0.46	0.46	

Fit 1, use splines to estimate both $\beta_l(t)$'s and α_1; Fit 2, use splines to estimate $\beta_l(t)$'s only. CP, coverage probability; SE, empirical standard error; SEM, mean of standard error.

under the low event rate setting. The corresponding coverage probabilities also display greater variation. However, in the high event rate setting, the mean estimates show negligible bias with the coverage probabilities more stable and close to the 95% nominal value.

Simulation results for the parametric coefficients are shown in Table 1. The $\hat{\phi}$ is approximate 2% smaller than the true value in the low event rate setting and 0.6% smaller than the true value in the high event rate setting. We assess the standard error estimation by comparing the mean of standard error (SEM, the average of estimated standard error) and the empirical standard error of the estimates (SE), which should be equal ideally. The SEM for $\hat{\phi}$ is 4% smaller than the SE under the setting of low-curvature time-varying coefficients and low event rate. For the rest of settings, the SEM and SE are similar.

The bias of $\hat{\phi}$ and the underestimation of standard error are consistent with the results of the work of Ripatti and Palmgren,[61] who used the PQL approximation in the inference procedure for multivariate frailty models. Since the uncertainty in the estimation of $\boldsymbol{\tau}$ is ignored when estimating the variances, the estimates tend to underestimate the true variances (see Equation (12) and the related discussion).

The mean estimate of α_1 has similar bias (2% smaller) in the low event rate setting, yet such bias is negligible in the high event rate setting. The bias in $\hat{\alpha}_1$ is connected to the bias in $\hat{\phi}$. The SEM for $\hat{\alpha}_1$ is very close to its SE, showing no underestimation. The coverage probability of the 95% confidence intervals for $\hat{\alpha}_1$ is close to or even slightly higher than the nominal level.

In summary, the simulation study shows the model provide satisfactory estimation for the true parameters in various settings. The biases of spline estimates and parametric coefficient estimates are small under both low and high event rates. The confidence intervals have close to nominal coverage probabilities. Although the frailty variance tends to be underestimated, the magnitude of the bias is limited.

4 | APPLICATION

We apply the proposed model to the Commercial Truck Driver NDS data. The objective is to evaluate the temporal profile of driving performance over long driving hours in a shift by the total sleep duration prior to the shift. The driving performance was measured by the ULD.

4.1 | Commercial Truck Driver NDS

The Commercial Truck Driver NDS[62] is a large-scale data collection study sponsored by the Federal Motor Carrier Safety Administration to evaluate issues related to commercial motor vehicles.

The study recruited 100 drivers from four for-hire trucking companies. Each driver drove an instrumented truck for approximately four weeks. The trucks were fitted with unobtrusive data-collection equipment, including four video cameras, radar, a global positioning system device, and kinematic sensors. Driving data were continuously recorded from ignition-on to ignition-off at high frequency, eg, 10 Hz for video, radar, and three-dimensional accelerometers. No

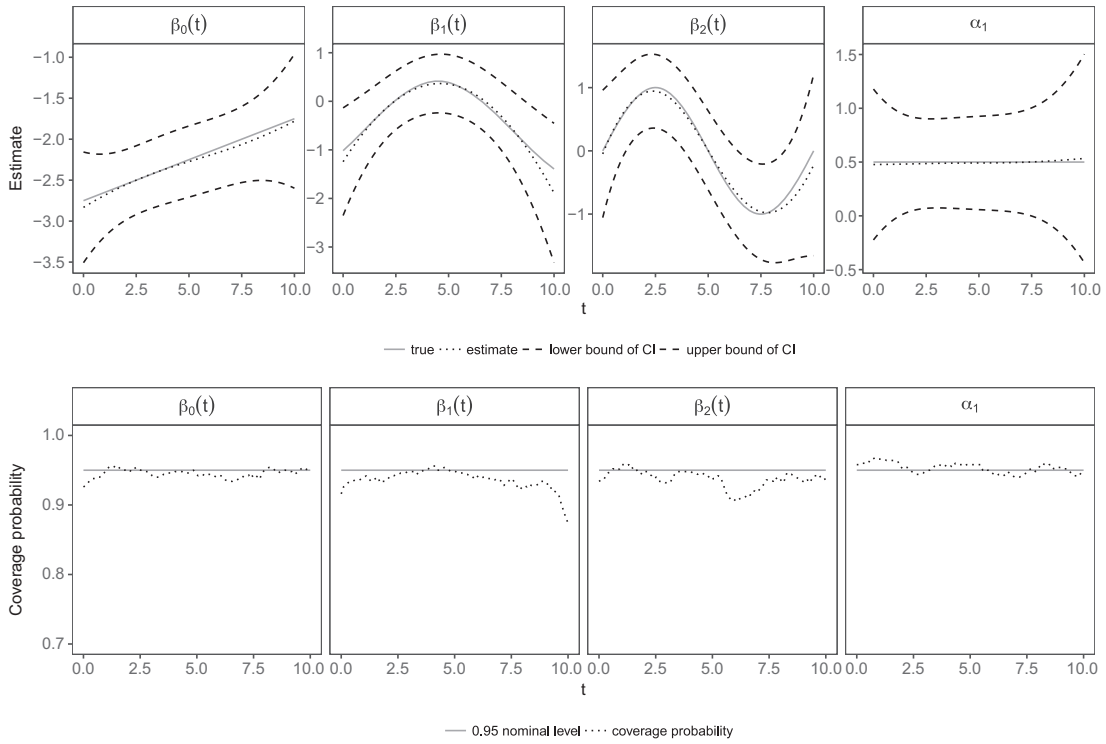

(1) Low event rate.

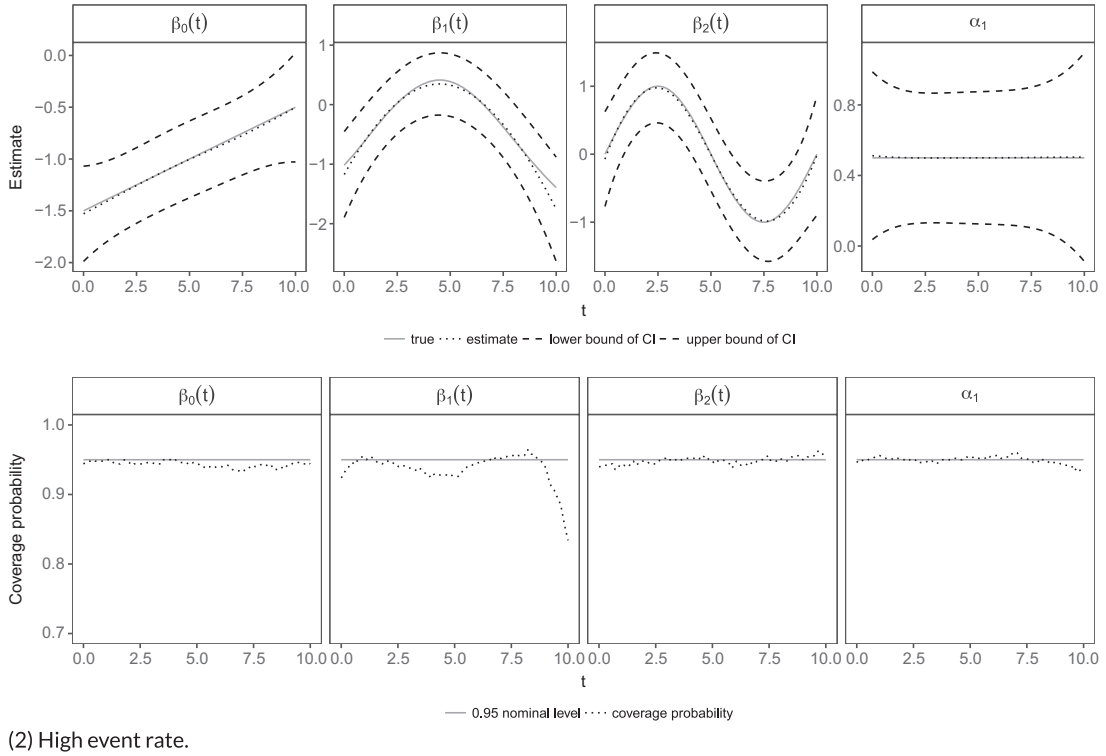

(2) High event rate.

FIGURE 1 Estimates, 95% confidence intervals (CIs) and coverage probability for the low-curvature time-varying coefficients simulation setting

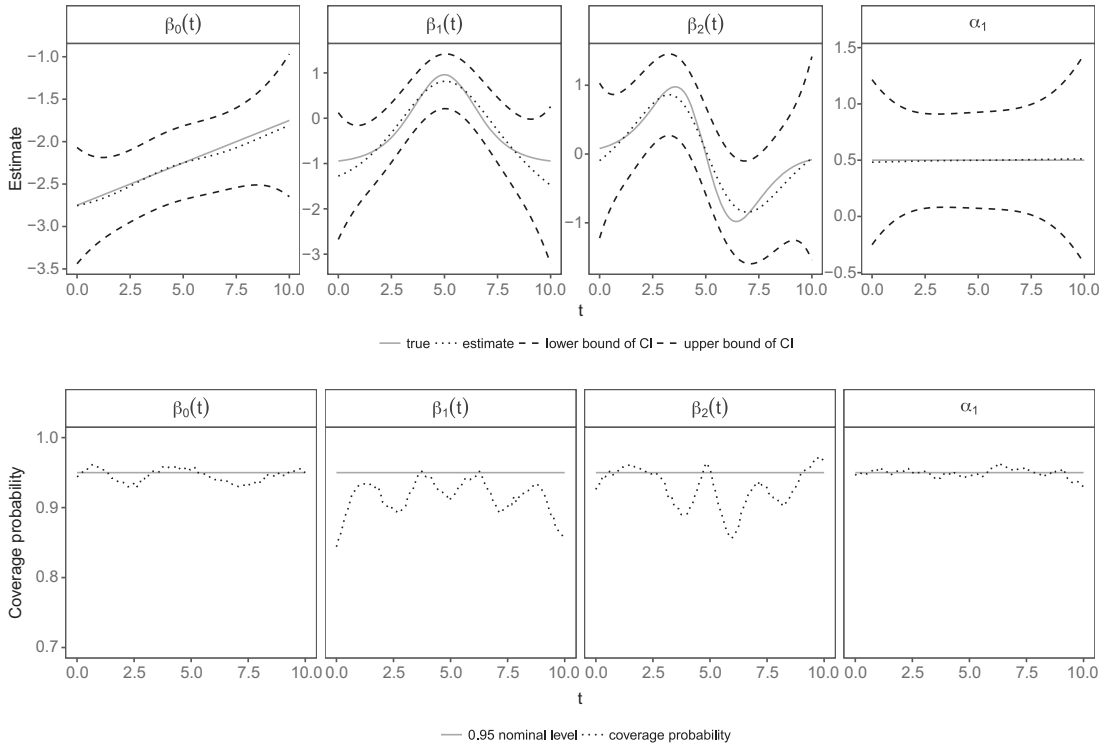

(1) Low event rate.

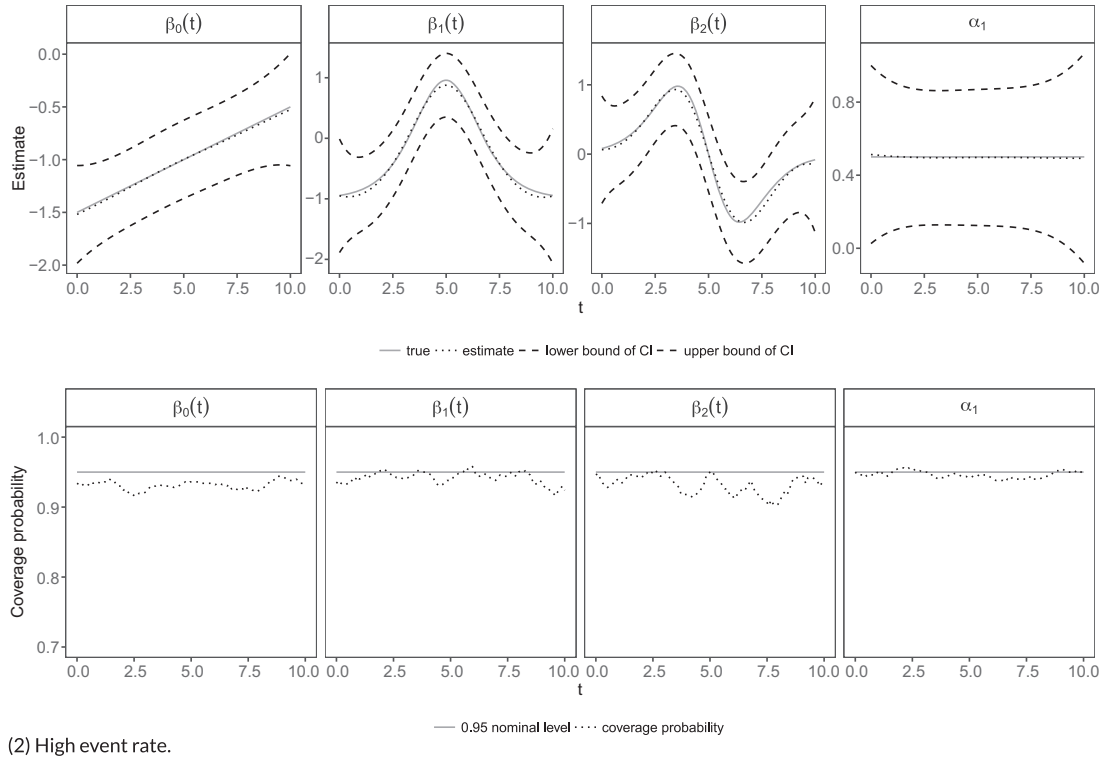

(2) High event rate.

FIGURE 2 Estimates, 95% confidence intervals (CIs) and coverage probability for the high-curvature time-varying coefficients simulation setting

specific instruction was given to the participants and the collected data thus present the naturalistic driving behavior under normal revenue generating driving activity.

The detailed driving data allow various driving behavior and performance to be examined. For this study, the ULD is selected as a measure of driving performance. The ULD is defined as "any circumstance where the subject vehicle crosses

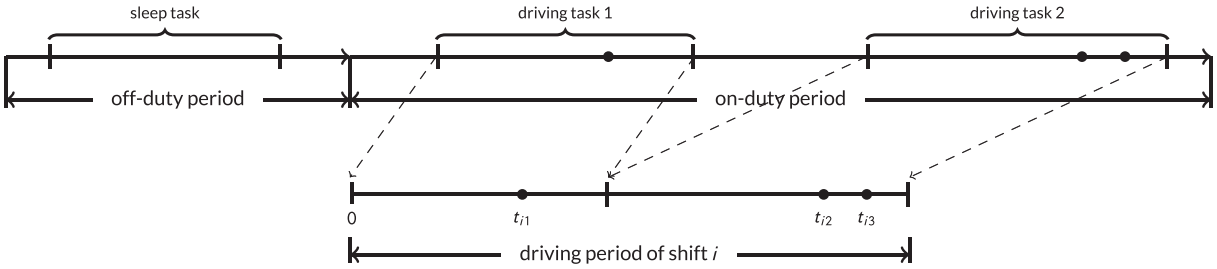

FIGURE 3 Illustration of data processing. Black dots represent unintentional lane deviation events, and t_{ij}, where $j = 1, 2, 3$, represents the driving time to event j in shift i

over a solid lane line (eg, on to the shoulder) where there is not a hazard (guardrail, ditch, vehicle, etc) present. In these cases, the driver does not signal or intentionally make a lane change maneuver" (see the work of Regan et al[63 p145]). Unintentional lane deviation has been shown to be a measure of driving performance decrement and sensitive to driving fatigue.[64,65]

The study also collected drivers' on-duty and off-duty activities through a daily activity register. The activity register includes information on working activities as well as activities related to fatigue, such as sleeping, loading, driving, as well as caffeine and drug use. The register also collects the beginning and ending times of each activity. The combination of NDS driving data and the activity register data provides a complete timeline of participants' driving and nondriving activities. To evaluate the impact of off-duty sleep time on drivers' subsequent on-duty driving performance, the data were organized into pairs of an off-duty period followed by an on-duty one. The analysis focus on the impact of total sleeping time in the off-duty period on the driver performance in the subsequent on-duty period. The daily schedules of commercial truck drivers are highly irregular. For example, some drivers opt to drive late at night to avoid traffic congestion and determine the on-duty status based on calendar time could be misleading. Another complication is that some participants failed to distinguish between on-duty and off-duty activity codes, eg, on-duty tasks were coded as off-duty and vice versa. To address these issues, the data were processed based on the following three criteria.

- Driving the truck, light work, and heavy work were considered on-duty tasks. Other tasks were considered off-duty.
- An off-duty period consisted of off-duty tasks only and met either of the two following criteria: (1) its total duration was 10 hours or longer (to be consistent with the HOS regulations that require at least 10 consecutive hours off duty for truck drivers to start a new on-duty shift); (2) it included at least 7 hours of sleep. The off-duty duration has to be reasonably long so that the beginning of a succeeding on-duty period is a "fresh start" for the driver.
- An on-duty period, which followed immediately after an off-duty one, consisted of on-duty tasks and potentially short off-duty tasks. An on-duty period longer than 14 hours was truncated (to be consistent with the 14-hour on-duty limit in the HOS regulations).

The procedure extracted 2056 on-duty periods, of which 2004 involved driving tasks. In each of these 2004 periods, episodes of driving tasks were connected in time to form the driving period of a shift (see Figure 3). The episodes between successive driving tasks were either breaks (eg, eat, rest, and sleep) or on-duty work (eg, loading, unloading). Due to the HOS regulations that require drivers to drive no more than 11 hours on-duty, driving longer than 11 hours in a shift was truncated. For each ULD event, the driving time to event from the beginning of the shift was calculated. Total sleep time from the preceding off-duty period was calculated. Since some off-duty periods involved multiple days or even weeks, sleep time within the 12-hour window right before an on-duty period was used. A total of 1880 shifts from 96 drivers contain valid sleep data and are included in the analysis.

4.2 | Characteristics of driving duration, ULDs, and breaks

The data contain 1880 off-duty and on-duty pairs from 96 drivers. To evaluate the impact of total sleep time, we group the shifts by total sleeping time in the off-duty period. Studies show that sleep time is generally considered insufficient if the total duration is less than 7 hours.[8-12] The off-duty sleep time is considered as normal if it is between 7 and 9 hours, and abundant if the duration is more than 9 hours. Among the 1880 shifts, 20.6% (388) are in the insufficient sleep time group, 58.2% (1095) in the normal sleep time group, and 21.1% (397) in the abundant sleep time group.

Table 2 compares the rate of ULD events by driving hour since a shift starts among the three sleep time groups. For each driving hour since the beginning of a shift, we calculated the number of ULDs occurred in the specific hour and the

TABLE 2 Unintentional lane deviations (ULDs) and driving exposure (hours) in the 1st to 11th driving hours by sleep time group

Driving time since a shift starts	Sleep hours ≤ 7			7 < Sleep hours ≤ 9			Sleep hours > 9		
	ULDs	Exposure	Rate	ULDs	Exposure	Rate	ULDs	Exposure	Rate
1*st* hour	21	384.11	0.055	52	1092.16	0.048	31	395.48	0.078
2*nd* hour	38	374.18	0.102	52	1078.64	0.048	31	392.78	0.079
3*rd* hour	13	371.50	0.035	60	1055.97	0.057	31	386.98	0.080
4*th* hour	14	360.58	0.039	106	1016.10	0.104	24	374.35	0.064
5*th* hour	33	333.32	0.099	83	970.26	0.086	20	358.31	0.056
6*th* hour	11	304.90	0.036	94	898.70	0.105	40	334.00	0.120
7*th* hour	24	251.49	0.095	96	781.78	0.123	36	301.14	0.120
8*th* hour	26	182.29	0.143	32	665.80	0.048	19	265.40	0.072
9*th* hour	19	130.99	0.145	40	547.23	0.073	14	228.44	0.061
10*th* hour	26	99.04	0.263	18	393.08	0.046	22	181.31	0.121
11*th* hour	10	61.60	0.162	8	267.69	0.030	22	130.49	0.169

Exposure in the *i*th hour, where $i = 1, \ldots, 11$, is the total driving time for all shifts that occurred in the *i*th hour. Rate is the ratio of ULDs to exposure.

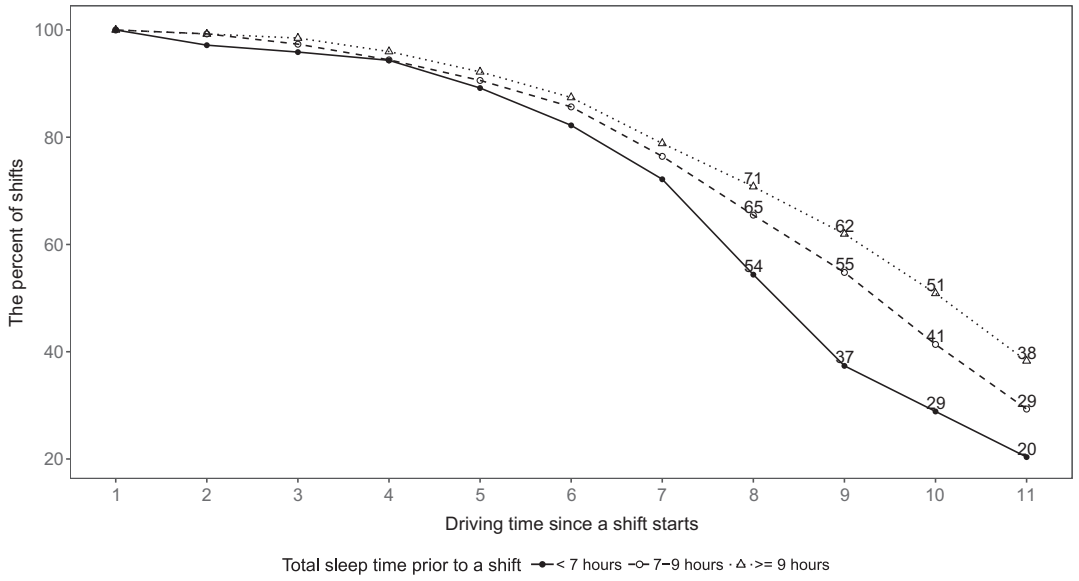

FIGURE 4 The percent of shifts driving into the 1st to 11th driving hour by sleep time group

exposure, ie, total driving time for all shifts that occurred in the specific hour. The event rate for a specific driving hour is a ratio of the ULD count over the driving exposure. As can be seen, the event rate for the insufficient sleep time group increases substantially after 8 hours of driving and reaches a peak of 0.26 in the 10th driving hour. The normal sleep time group, ie, sleep time between 7 and 9 hours, observes no substantial increase at later hours of driving. The event rate of the abundant group increased considerably in the 10th hour of driving. These results suggest that temporal profile of the ULD event rates vary substantially by sleep time groups. The group with insufficient sleep time (< 7 hours) tend to have a higher ULD rate in the later driving part of a shift.

Analysis shows that the sleep time prior to a shift is related to the driving length of a shift. The mean driving length for shifts with insufficient sleep time is 7.36 hours, for normal sleep time group is 8.01 hours, and for abundant sleep time group is 8.43 hours. A statistically significant correlation can be found between total driving length and sleep time. Figure 4 shows the percent of shifts driving into the 1st to 11th driving hour for each sleep time group. The shifts with abundant sleep time has the highest percentage of driving in each of the 11 hours, followed by the normal sleep time group, and the insufficient group has the lowest percentage. The abundant group has 38% of shifts driving into the 11th driving hour, the normal group has 29%, while the insufficient group has only 20%. This implies drivers' self-selection in terms of taking sufficient sleep prior to a long shift or shortening driving time with insufficient sleep.

Studies have shown that breaks during long driving periods could also affect the subsequent driving performance.[15] Figure 5 compares the ratios of break length to driving exposure among the three sleep time groups. For the *i*th hour

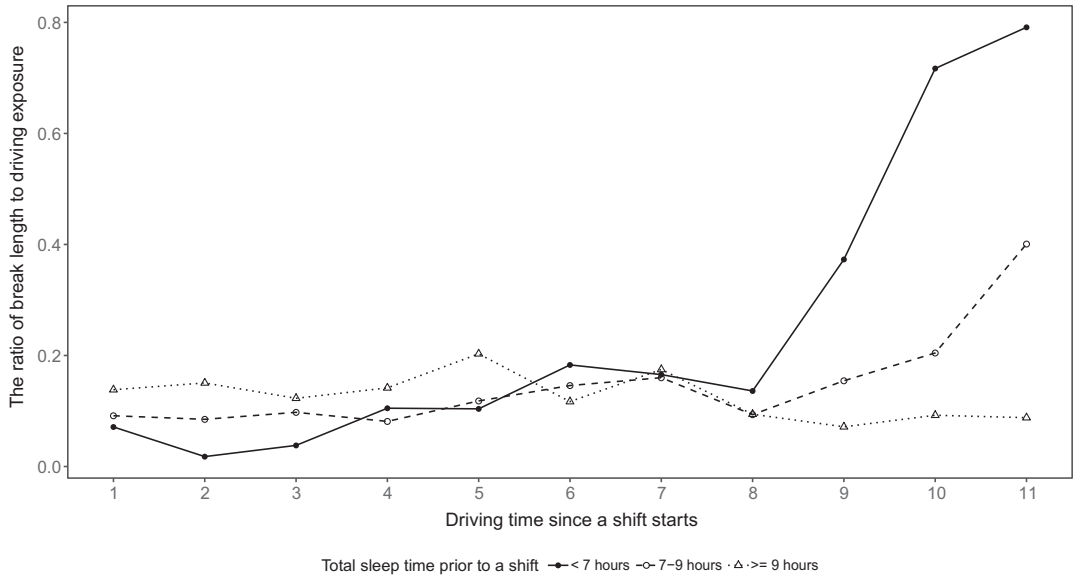

FIGURE 5 The ratio of break length (in hours) to driving exposure (in hours) in the 1st to 11th driving hours by sleep time group

since a shift starts, where $i = 1, \ldots, 11$, the break duration is the sum of break duration from all shifts in the ith hour of driving. The ratio of the break duration over the driving exposure for the ith hour represents the average length of breaks for every hour of driving. As shown in Figure 5, in the first 8 driving hours, the ratios for all three groups are stably below 0.2. Starting from the 8th driving hour, the difference becomes substantial, ie, the ratio for insufficient sleep time climbs rapidly and reaches the maximum of 0.8 in the 11th driving hour; the ratio for normal sleep time has a slower increasing trend and reaches its maximum of 0.4 at the end; the abundant group stays constantly low around 0.1. This result indicates that drivers who slept less tended to take longer breaks in the later driving part of a shift.

4.3 | Assessing driving performance profile over time using the time-varying coefficient model

We applied the proposed time-varying coefficient model to the Commercial Truck Driver NDS data. Two dummy variables were created to represent the three sleep time groups. The coefficients for these two dummy variables were assumed to be time-varying. The log baseline (normal sleep time) intensity and the time-varying coefficients were modeled by cubic B-splines with the number of knots $k_l = 10$ and the order of difference penalty $r = 3$. The results show that the estimate of the frailty variance is $\hat{\phi} = 7.68$ and its standard error is 0.59.

Figure 6 shows the estimates for time-varying coefficients. The time-varying coefficient of the insufficient indicator variable gives a temporal profile of the difference between the insufficient and normal sleep time groups. Starting from the 8th driving hour, the coefficient function is above zero and keeps increasing as driving time increases. This indicates that the intensity of ULD for the insufficient and normal sleep time groups is similar for the first 8 hours of driving. After 8 hours, shifts with insufficient sleep time have a higher intensity than those with normal sleep time. The difference keeps increasing with driving hours. Similar pattern was observed for the difference between the abundant and normal sleep time groups. The shifts with abundant sleep time show a significant higher intensity after 8 hours of driving hour.

Figure 7 displays the estimated intensities for the three sleep time groups. The intensity for insufficient sleep time stays low in the first 6 driving hours and then starts to increase. The intensity for normal sleep time slowly climbs up and reaches the peak around the 5th driving hour, after that the function declines as time goes on. The intensity for abundant sleep time remains constant over the whole driving time.

The results indicate that shifts with normal sleep time show a lower intensity compared to both insufficient and abundant sleep time. While the higher intensity for shifts with insufficient is expected, it is counterintuitive that the abundant sleep group also shows a higher intensity. As many factors could affect driving performance, this result could be results of other factors, eg, the characteristics of breaks described in Section 4.2. As shown in Figure 7, the ratio of break length to driving exposure for normal sleep time starts to increase from the 8th hour of driving. On the contrary, the abundant group has a low break ratio over the entire driving time. The shorter break length at later part of a shift for the abundant sleep time group could be a potential reason for the high ULD intensity.

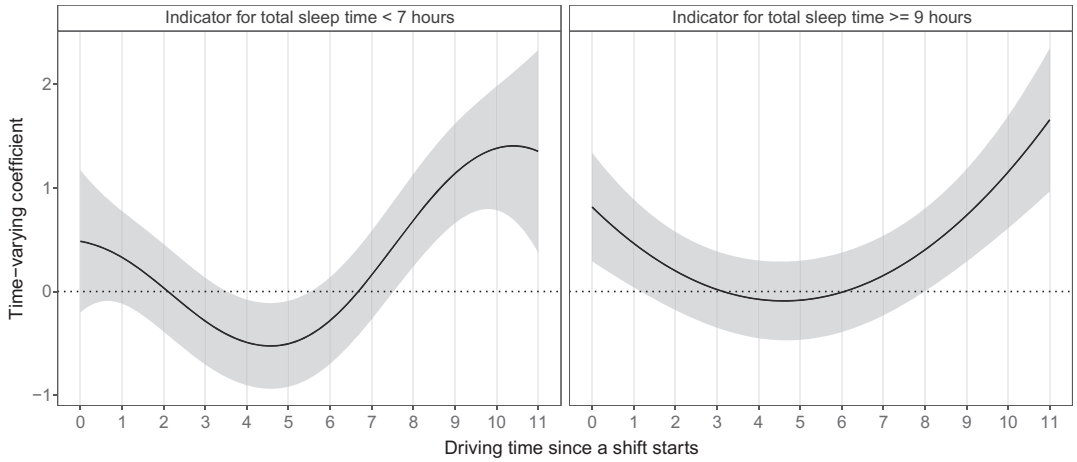

FIGURE 6 The time-varying coefficients: spline estimate (in solid line) and 95% pointwise confidence interval (in shaded area)

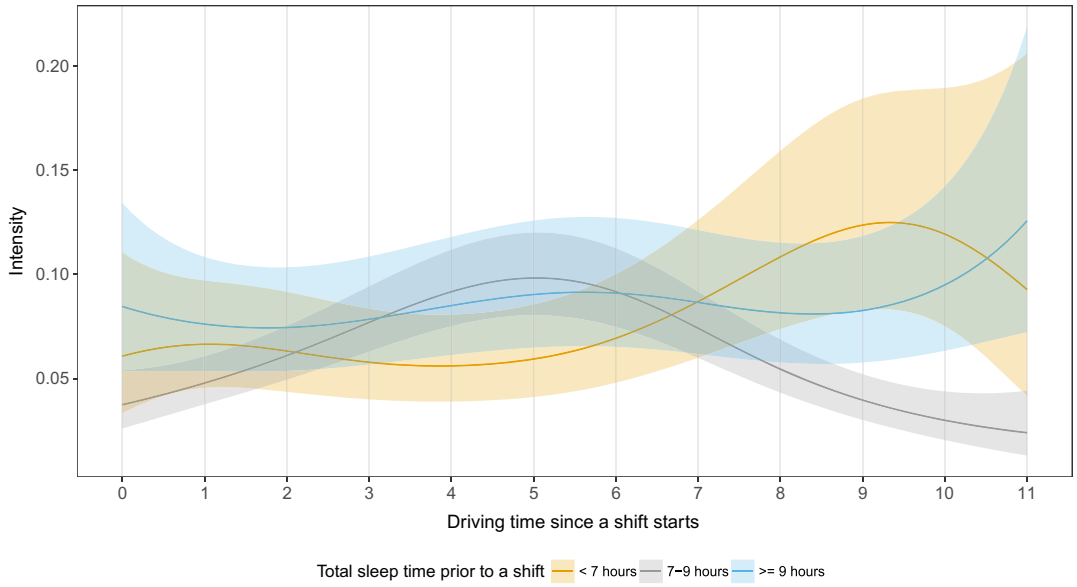

FIGURE 7 The intensity by sleep time group: spline estimate (in solid line) and 95% pointwise confidence interval (in shaded area) [Colour figure can be viewed at wileyonlinelibrary.com]

The difference between insufficient and normal sleep time is most pronounced. From the 8th driving hour, drivers with insufficient sleep time have the highest break ratio, taking breaks of more than half an hour for every hour of driving. However, in the same time range, the associated coefficient function rises above zero and increases rapidly (see Figure 6). This implies that, compared to normal sleep time, drivers with insufficient sleep time tend to take considerably longer breaks after 8 hours of driving, yet these substantial amount of breaks could not prevent a higher intensity; their gap is even wider as the driving continues. The result implies that longer break in later part of a shift is not sufficient to compensate lack of sleep prior to the shift.

5 | DISCUSSION

Fatigue is a major issue associated with commercial truck drivers, especially long-haul truck drivers who may work 14 hours, and drive 11 hours in a single shift. A recent report by the National Academies acknowledges the hazard of fatigue and suggests that research needs to be conducted to understand the impact of fatigue on the safety and health of truck drivers.[3] However, there is limited research on how fatigue affects drivers' performance using high-resolution in situ

collected driving data. This study advances the research in understanding driving fatigue by evaluating the time-varying effects of total sleep time prior to a shift using the proposed model.

We propose a mixed Poisson process model with time-varying coefficients for recurrent event data. Gamma frailties are incorporated to accommodate the dependence among event times. A mixed-model representation of penalized splines is adopted for modeling both the log baseline intensity and time-varying coefficients. An EM algorithm is used to fit the model, in which the PQL approach is adopted for likelihood approximation. The simulation study has confirmed that the model performs well for time-varying coefficients with different degrees of curvature under both low and high event rate scenarios. In this paper, we use a gamma frailty to model the correlation between event times. As suggested by a reviewer, we evaluated our estimates in the settings where the random effect was generated from a log normal distribution but was modeled to be gamma in the simulation study. We found that our model still performed reasonably well in that the spline estimates for both time-varying and constant coefficients had very little bias.

There are several possible extensions of the current research. This paper uses a frailty term for shift-level heterogeneity in the data. However, heterogeneity may also exist at the driver level.[24] A nested frailty model with random effects for both levels is worth pursuing yet requires a larger sample size. The gamma frailty assumption used in this paper can be relaxed through the nonparametric frailty in future studies.[66-68] To account for the correlation structure between event times, an alternative is to use generalized estimating equations.[69,70] In addition, many factors could contribute to driving performance, eg, caffeine intake, breaks and rest, as well as time of day. Certain seemly unusual patterns observed in the results, eg, high ULD intensity for abundant sleep group after 9 hours of driving could be associated the short break and rest for this cohort. How to incorporate or adjust these factors is worth investigating.

The application results reveal that lack of sleep primarily affects driving performance, as measured by ULDs, after 8 hours of driving in a given shift. That is, the negative impacts of insufficient sleep are most apparent in terms of performance decrement well into the driver's shift. The results also implies a complex relationship among total sleep time, the driver's choice to take breaks while on duty, and driving performance. Compared to normal sleep time, drivers with insufficient sleep tend to take markedly more breaks after 8 hours of driving, yet these extra breaks could not prevent a higher risk; their gap is even wider as the driving continues. This highlights the importance of drivers beginning their shift well-rested and having sufficient sleep the night before driving. Furthermore, a driver's fitness-to-drive, in terms of increased safety risk while on the road, can be assessed, in part, by measuring how much sleep the driver received prior to beginning the shift. The finding that a performance decrement appears after 8 hours into the shift also provides important information for technology developers aimed at fatigue detection, and for those interested in determining the role that fatigue may play in a road crash.

DATA AVAILABILITY STATEMENT

The data that support the findings of this study are available on request from the corresponding author. The data are not publicly available due to privacy or ethical restrictions.

ORCID


Feng Guo https://orcid.org/0000-0002-2572-481X

REFERENCES

1. Federal Motor Carrier Safety Administration. Large truck and bus crash facts 2015. Washington, DC: Federal Motor Carrier Safety Administration; 2016.
2. Federal Motor Carrier Safety Administration. Hours of service of drivers. *Federal Register*. 2011;76(248):81134-81188.
3. National Academies of Sciences, Engineering, and Medicine. *Commercial Motor Vehicle Driver Fatigue, Long-Term Health, and Highway Safety: Research Needs*. Washington, DC: The National Academies Press; 2016.
4. Banks S, Dinges DF. Behavioral and physiological consequences of sleep restriction. *J Clin Sleep Med*. 2007;3(5):519-528.
5. Hanowski R, Hickman J, Fumero MC, Olson RL, Dingus TA. The sleep of commercial vehicle drivers under the 2003 hours-of-service regulations. *Accid Anal Prev*. 2007;39(6):1140-1145.
6. Lim J, Dinges DF. Sleep deprivation and vigilant attention. *Ann N Y Acad Sci*. 2008;1129(1):305-322.
7. Lim J, Dinges DF. A meta-analysis of the impact of short-term sleep deprivation on cognitive variables. *Psychological Bulletin*. 2010;136(3):375-389.
8. Van Dongen HPA, Maislin G, Mullington JM, Dinges DF. The cumulative cost of additional wakefulness: dose-response effects on neurobehavioral functions and sleep physiology from chronic sleep restriction and total sleep deprivation. *Sleep*. 2003;26(2):117-126.

9. Van Dongen HPA, Rogers NL, Dinges DF. Sleep debt: theoretical and empirical issues. *Sleep Biol Rhythms*. 2003;1(1):5-13.
10. Ford ES, Cunningham TJ, Croft JB. Trends in self-reported sleep duration among US adults from 1985 to 2012. *Sleep*. 2015;38(5):829-832.
11. Watson NF, Badr MS, Belenky G, et al. Joint consensus statement of the American Academy of Sleep Medicine and Sleep Research Society on the recommended amount of sleep for a healthy adult: methodology and discussion. *Sleep*. 2015;38(8):1161-1183.
12. Watson NF, Badr MS, Belenky G, et al. Recommended amount of sleep for a healthy adult: a joint consensus statement of the American Academy of Sleep Medicine and Sleep Research Society. *Sleep*. 2015;38(6):843-844.
13. Abe T, Komada Y, Inoue Y. Short sleep duration, snoring and subjective sleep insufficiency are independent factors associated with both falling asleep and feeling sleepiness while driving. *Internal Medicine*. 2012;51(23):3253-3260.
14. Scott LD, Hwang W-T, Rogers AE, Nysse T, Dean GE, Dinges DF. The relationship between nurse work schedules, sleep duration, and drowsy driving. *Sleep*. 2007;30(12):1801-1807.
15. Soccolich SA, Blanco M, Hanowski RJ, et al. An analysis of driving and working hour on commercial motor vehicle driver safety using naturalistic data collection. *Accid Anal Prev*. 2013;58:249-258.
16. Albert PS. Driving the analysis: an exciting opportunity for statistical innovation in driving research. *Statist Med*. 2019;38(2):151.
17. Dawson JD. Practical and statistical challenges in driving research. *Statist Med*. 2019;38(2):152-159.
18. Simons-Morton B. Driving in search of analyses. *Statist Med*. 2017;36(24):3763-3771.
19. Klauer SG, Guo F, Simons-Morton BG, Ouimet MC, Lee SE, Dingus TA. Distracted driving and risk of road crashes among novice and experienced drivers. *N Engl J Med*. 2014;370(1):54-59.
20. Dingus TA, Guo F, Lee S, et al. Driver crash risk factors and prevalence evaluation using naturalistic driving data. *Proc Natl Acad Sci USA*. 2016;113(10):2636-2641.
21. Guo F, Klauer SG, Fang Y, et al. The effects of age on crash risk associated with driver distraction. *Int J Epidemiol*. 2017;46(1):258-265.
22. *National Motor Vehicle Crash Causation Survey: Report to Congress*. National Highway Traffic Administration, 2008, Report No. DOT HS 811 059.
23. Guo F. Statistical methods for naturalistic driving studies. *Annu Rev Stat Appl*. 2019;6:309-328.
24. Kim S, Chen Z, Zhang Z, Simons-Morton BG, Albert PS. Bayesian hierarchical Poisson regression models: an application to a driving study with kinematic events. *J Am Stat Assoc*. 2013;108(502):494-503.
25. Guo F, Kim I, Klauer SG. Semiparametric Bayesian models for evaluating time-variant driving risk factors using naturalistic driving data and case-crossover approach. *Statist Med*. 2019;38(2):160-174.
26. Byar D, Blackard C; The Veterans Administration Cooperative Urological Research Group. Comparisons of placebo, pyridoxine, and topical thiotepa in preventing recurrence of stage I bladder cancer. *Urology*. 1977;10(6):556-561.
27. Gail MH, Santner TJ, Brown CC. An analysis of comparative carcinogenesis experiments based on multiple times to tumor. *Biometrics*. 1980;36(2):255-266.
28. Therneau TM, Hamilton SA. rhDNase as an example of recurrent event analysis. *Statist Med*. 1997;16(18):2029-2047.
29. Pepe MS, Cai J. Some graphical displays and marginal regression analyses for recurrent failure times and time dependent covariates. *J Am Stat Assoc*. 1993;88(423):811-820.
30. Lawless JF, Nadeau C. Some simple robust methods for the analysis of recurrent events. *Technometrics*. 1995;37(2):158-168.
31. Lin DY, Wei LJ, Yang I, Ying Z. Semiparametric regression for the mean and rate functions of recurrent events. *J R Stat Soc Ser B Stat Methodol*. 2000;62(4):711-730.
32. Lawless JF. Regression methods for Poisson process data. *J Am Stat Assoc*. 1987;82(399):808-815.
33. Nielsen GG, Gill RD, Andersen PK, Sørensen TI. A counting process approach to maximum likelihood estimation in frailty models. *Scand J Stat*. 1992;19:25-43.
34. Vaida F, Xu R. Proportional hazards model with random effects. *Statist Med*. 2000;19(24):3309-3324.
35. Guo F, Klauer SG, Hankey JM, Dingus TA. Near crashes as crash surrogate for naturalistic driving studies. *Transp Res Rec*. 2010;2147(1):66-74.
36. Guo F, Fang Y. Individual driver risk assessment using naturalistic driving data. *Accid Anal Prev*. 2013;61:3-9.
37. Olson RL, Hanowski RJ, Hickman JS, Bocanegra J. *Driver Distraction in Commercial Vehicle Operations*. Technical report. Washington, DC: Federal Motor Carrier Safety Administration; 2009.
38. Chen C, Guo F. Evaluating the influence of crashes on driving risk using recurrent event models and naturalistic driving study data. *J Appl Stat*. 2016;43(12):2225-2238.
39. Li Q, Guo F, Klauer SG, Simons-Morton BG. Evaluation of risk change-point for novice teenage drivers. *Accid Anal Prev*. 2017;108:139-146.
40. Li Q, Guo F, Kim I, Klauer SG, Simons-Morton BG. A Bayesian finite mixture change-point model for assessing the risk of novice teenage drivers. *J Appl Stat*. 2018;45(4):604-625.
41. Carroll RJ, Ruppert D, Welsh AH. Local estimating equations. *J Am Stat Assoc*. 1998;93(441):214-227.
42. Cai Z, Fan J, Li R. Efficient estimation and inferences for varying-coefficient models. *J Am Stat Assoc*. 2000;95(451):888-902.
43. Hastie T, Tibshirani R. Varying-coefficient models. *J R Stat Soc Ser B Stat Methodol*. 1993;55(4):757-779.
44. Hastie T, Loader C. Local regression: automatic kernel carpentry. *Stat sci*. 1993;8(2):120-129.
45. Eilers PHC, Marx BD. Flexible smoothing with B-splines and penalties. *Stat sci*. 1996;11(2):89-102.
46. Amorim LD, Cai J, Zeng D, Barreto ML. Regression splines in the time-dependent coefficient rates model for recurrent event data. *Statist Med*. 2008;27(28):5890-5906.
47. Sun L, Zhou X, Guo S. Marginal regression models with time-varying coefficients for recurrent event data. *Statist Med*. 2011;30(18):2265-2277.

48. Yu Z, Liu L, Bravata DM, Williams LS, Tepper RS. A semiparametric recurrent events model with time-varying coefficients. *Statist Med*. 2013;32(6):1016-1026.
49. Cox DR. Partial likelihood. *Biometrika*. 1975;62(2):269-276.
50. Brumback BA, Rice JA. Smoothing spline models for the analysis of nested and crossed samples of curves. *J Am Stat Assoc*. 1998;93(443):961-976.
51. Wang Y. Mixed effects smoothing spline analysis of variance. *J R Stat Soc Ser B Stat Methodol*. 1998;60(1):159-174.
52. Wang Y. Smoothing spline models with correlated random errors. *J Am Stat Assoc*. 1998;93(441):341-348.
53. Brumback BA, Ruppert D, Wand MP. Variable selection and function estimation in additive nonparametric regression using a data-based prior: comment. *J Am Stat Assoc*. 1999;94(447):794-797.
54. Breslow NE, Clayton DG. Approximate inference in generalized linear mixed models. *J Am Stat Assoc*. 1993;88(421):9-25.
55. Cai T, Hyndman RJ, Wand MP. Mixed model-based hazard estimation. *J Comput Graph Stat*. 2002;11(4):784-798.
56. Cai T, Betensky RA. Hazard regression for interval-censored data with penalized spline. *Biometrics*. 2003;59(3):570-579.
57. Berry SM, Carroll RJ, Ruppert D. Bayesian smoothing and regression splines for measurement error problems. *J Am Stat Assoc*. 2002;97(457):160-169.
58. Lang S, Brezger A. Bayesian P-splines. *J Comput Graph Stat*. 2004;13(1):183-212.
59. Tierney L, Kadane JB. Accurate approximations for posterior moments and marginal densities. *J Am Stat Assoc*. 1986;81(393):82-86.
60. Gray RJ. Flexible methods for analyzing survival data using splines, with applications to breast cancer prognosis. *J Am Stat Assoc*. 1992;87(420):942-951.
61. Ripatti S, Palmgren J. Estimation of multivariate frailty models using penalized partial likelihood. *Biometrics*. 2000;56(4):1016-1022.
62. Blanco M, Hanowski RJ, Olson RL, et al. *The Impact of Driving, Non-Driving Work, and Rest Breaks on Driving Performance in Commercial Motor Vehicle Operations*. Technical report. Washington, DC: Federal Motor Carrier Safety Administration; 2011.
63. Regan MA, Lee JD, Victor TW. *Driver Distraction and Inattention: Advances in Research and Countermeasures, Volume 1*. London, UK: CRC Press; 2017.
64. Hanowski RJ, Bowman D, Alden A, Wierwille WW, Carroll R. *PERCLOS+: Moving Beyond Single-Metric Drowsiness Monitors*. SAE technical paper; 2008.
65. Van Dongen HPA, Jackson ML, Belenky G. *Duration of Restart Period Needed to Recycle With Optimal Performance: Phase II*. Technical report. Washington, DC: Federal Motor Carrier Safety Administration; 2010.
66. Fan J. On the optimal rates of convergence for nonparametric deconvolution problems. *Ann Stat*. 1991;19(3):1257-1272.
67. Chen J. Optimal rate of convergence for finite mixture models. *Ann Stat*. 1995;23(1):221-233.
68. Carroll RJ, Hall P. Optimal rates of convergence for deconvolving a density. *J Am Stat Assoc*. 1988;83(404):1184-1186.
69. Zeger SL, Liang K-Y. An overview of methods for the analysis of longitudinal data. *Statist Med*. 1992;11(14-15):1825-1839.
70. Lipsitz SR, Laird NM, Harrington DP. Generalized estimating equations for correlated binary data: using the odds ratio as a measure of association. *Biometrika*. 1991;78(1):153-160.

How to cite this article: Liu Y, Guo F, Hanowski RJ. Assessing the impact of sleep time on truck driver performance using a recurrent event model. *Statistics in Medicine*. 2019;1–16. https://doi.org/10.1002/sim.8287